Exploremetics
Journal of Innovative Engineering and Technology

Volume: 07 No: 02 | August -2026
ISSN (Online) 2636 – 590
ISSN (Print) 2636 - 591X

OPTIMIZATION OF VULCANIZATION PROCESS USING PALMYRA PALM FIBER

Ekete Juliet Azuka[*1], Eze Kenneth Afamefuna[1], Aliozo Sandra Ogechukwu[1]
1 Department of Chemical Engineering, Enugu State University of Science and Technology, Agbani, Enugu.
Author for Correspondence: Ekete J.A; **Email**: juliet.ekete@esut.edu.ng

Abstract - Optimization of the vulcanization process using Palmyra palm fiber is the focus of this study. It was performed using Design-Expert 8.0.7.1 trial version to maximize the vulcanization process parameters. The simultaneous effects of process variables such as time (7-10 minutes), temperature (140-160ºC), and fiber length (short and long) were evaluated. Response surface methodology (RSM) based on central composite design (CCD) was employed to optimize the vulcanization process. To correlate the vulcanization process variables with the responses, such as tensile strength, elongation at break, and modulus of elongation at 100%, quadratic models were created based on the CCD. The models were then examined using the proper statistical techniques. The predicted values and the actual experimental values were found to be in good agreement. As such, statistical analysis revealed that all of the designed models were found to be appropriate for the prediction of the corresponding reactions. The best process parameters for the highest tensile strength were determined to be 5.05261 MPa, elongation at break, 721.739%, modulus at 100% elongation, 0.728254 MPa at 7.00 minutes, 150ºC, and long fiber length. The generated model was validated, and optimum parameters were obtained as 5.4Mpa tensile strength, 739% elongation at break, and 0.7Mpa modulus at100% elongation.

Keywords: Natural rubber, optimization, Palmyra palm fiber

1. INTRODUCTION

Over a century ago, researchers began looking for ways to improve the characteristics and processing of rubber. Adding additives to the polymer matrix is one method of extending the rubber's service life (Nwabanne et al., 2015). Additives are substances that, when added to a polymer base, facilitate processing, lower product costs, and improve service qualities. (Darina et al. 2018, Abdelaal et al. 2021). Filler has a significant impact on rubber material and is one of the main additions used in natural rubber compounds (Nabeel and Ahmad, 2021).

Natural rubber vulcanizate's physico-mechanical and, to some degree, chemical properties are altered by filler (Hema et al. 2017, Chai et al. 2016). The process of vulcanization turns raw rubber, which is primarily thermoplastic, into an elastic or rigid condition that resembles ebonite. This procedure, which is often referred to as "cross-linking" or "curing," entails the joining of macromolecules through their reactive sites. Rubber's cross-linking gives it a number of characteristics. It becomes more resistant to chemical attack, increases its tensile strength, and is no longer rubber or thermoplastic. Additionally, it smooths the material's surface, keeps it from adhering to metal or plastic chemical catalysts, and makes it impermeable to moderate heat and cold. It also acts as an excellent insulator against heat and electricity. (Hossein et al. 2022, Haslilywaty et al. 2018). The objectives of this work include varying the time, temperature, and fiber length of Palmyra palm fiber filler to obtain the best vulcanization condition using Palmyra palm fiber. In order to optimize the tensile strength, elongation at break, and modulus at 100%

elongation of vulcanized rubber packed with Palmyra palm fiber. It employed response surface methodology, a set of mathematical and statistical methods. The objective of the study was to maximize the vulcanization process parameters of natural rubber using Palmyra palm fiber as a filler additive.

2.0 EXPERIMENTAL

2.1 Materials

The Palmyra palm fruits were collected from Nnamdi Azikiwe University, Awka, Anambra State, and processed to get Palmyra palm fiber. The Rubber Research Institute of Nigeria, located in Iyanomo, Benin City, Edo State, Nigeria, provided the natural rubber (NR) crumb of grade standard Nigerian rubber (SNR10), which also complies with Technically Specified Rubber (TSR-10), needed for this project. The compounded constituents and additives included zinc oxide, processing oil, stearic acid, carbon black (N330), sulfur, trimethyl quinoline (TMQ), and mercaptobenzoylthiazole (MBT). These commercial-grade compounding agents were acquired from Jonaz Industrial Chemicals, Stinpex Chemicals, and Ally Industrial Chemicals in Benin, Edo State, Nigeria.

2.2 Fiber preparation

The crude fibers are obtained from the ripe Palmyra palm fruits collected from Nnamdi Azikiwe University, Awka, Anambra State. The Palmyra palm fruits were retted and the fibers extracted, washed, and sun-dried.

2.2.1 Fiber Surface Treatment

Alkali and saline treatments were jointly used in the treatment process. These treatments were chosen because they have been shown to improve mechanical and interfacial strength with epoxy matrices (Keolebogile et al., 2022).

2.2.2 Alkaline Treatment

As used in previous reports (Kumarjyoti et al., 2020; Chimekwene et al., 2012), the standard method of alkaline treatment was adopted. In order to maintain a liquor ratio of 20:1 (by weight), pre-dried Palmyra palm fibers were soaked in a 1 M sodium hydroxide (NaOH) solution at room temperature. For thirty minutes, the fibers were submerged in the solution. The fibers were neutralized with a 1% acetic acid solution after being thoroughly cleaned with water to get rid of any remaining alkali on their surface. Following a 12-hour air-drying period, the treated fibers were dried for eight hours at 60 degrees Celsius in an oven.

2.2.3 Silane Treatment

Since acetone encourages hydrolysis, a solution of 0.5wt% saline coupling agent [3-(2-aminoethyl amino) aminopropyltrimethoxysilane was made for the treatment. After adding acetic acid to bring the solution's pH down to 5.5, it was constantly agitated for five minutes. After being treated in the alkali solution, the fibers were submerged in the saline solution for forty-five minutes. After removing chemical residues with acetone and water until the pH reached 7, the fibers were dried for 24 hours at 70 degrees Celsius in an oven. All fibers that had previously undergone alkali treatment were subjected to this silane process. The fibers were blended following standard treatment procedures (Chimekwene et al., 2012; Qianting et al., 2020)

2.3 Fiber characterization

Characterization was done in two phases: (i) physico-chemical analysis of the fiber and (ii) instrumental analysis using a Fourier Transform Infrared Spectrophotometer (FTIR) to determine the constituents of the Palmyra palm fiber used. pH, loss on ignition, conductivity, bulk density, acid-soluble lignin, ash content, moisture content, cellulose, hemicellulose, and lignin were all measured for the untreated, treated, and CB (N330). According to Hyman et al, 2008) and (Anup Kumar B. et al. 2023), these parameters were ascertained using the proper standard methods, and the results are presented in Table 2.

2.4 Fiber Blending/Sieving

The treated fibers were blended in an electric blender immediately after drying. The blended fibers were sieved into different mesh sizes with A.S.T.M. E.11 specification, the U.S.A. standard testing sieve comprising 600, 250, and 75µm. The essence of the sieving is to get the required particle size comparable to the

size of conventional carbon black used in rubber compounding. After sieving, the samples were stored in desiccators to avoid moisture absorption. Afterward, the fibers were then weighed into the required volume ratios for the compounding operation.

2.5 Compounding

Table 1 provides the formulation that was utilized to compound the natural rubber. In order to prevent cross-linking, the ingredients were mixed in a 160 x 320 mm two-roll mill with an attached water cooling system that kept the temperature below 80 degrees Celsius. The Monsanto Rheometer (ALPHA ODR 2000 Model, manufactured in Germany) was used to measure the cure qualities in compliance with the ASTM 3814 standard. The test pieces were cured by compression molding at a temperature of 160 degrees Celsius and a pressure of 150 kPa in a steam-heated hydraulic press. The test specimens were vulcanized using the cure times anticipated by the Mosanto rheographs as a guide.

Table 1. The formulation for carbon black/Palmyra palm fiber as fillers in natural rubber compounding.

Ingredients	**Phr**							
Natural rubber	100							
Stearic Acid	2							
Zinc oxide	5							
TMQ	1							
MBT	1							
Sulphur	2							
Processing oil	2							
Carbon black	0	10	20	30	40	50	60	70
Palmyra palm filler	70	60	50	40	30	20	10	0

TMQ: Trimethyl quinoline, MBT: Mercaptobenzoyl thiazole.

2.6 Experimental Design using Central Composite Design (CCD)

In order to optimize the vulcanization process, with replicates at the center point, an ideal design consisting of two numerical and one categorical factor CCD was employed. The factors under investigation were vulcanization time (A), temperature (B), and fiber length (C). The short fiber length has an average length of 5cm while that of long length has an average length of 10cm. The initial trials served as the basis for choosing the variable ranges. Equation (1) was used to determine the number of experiments needed for a three-variable CCD.

$$N=2^n + 2n + n_c \qquad (1)$$

In Equation (1), n is the number of independent variables. The numbers of factorial and axial points are represented by the first term (2^n) and the second term (2n), respectively, while the number of replicates at the center point is denoted by the third term (nc). Eight factorial points, eight axial points, and ten replicates at the center point make up the 26 experiments of the entire CCD design of this study. The experiment's repeatability and reliability were assessed using the center point replicates process. Table 1 lists the range of variables and their levels that were examined. The center point of the design is represented by zero, while the variables coded as −1 and +1 indicate the low and high levels of the variables under study. The software Design Expert 8.0.7.1 (trial version, Stat-Ease Inc., Minneapolis, MN, USA) was used to create the entire CCD design. Table 2 displays the entire design matrix that was produced using the coded and explicit independent variables together with the related retorts. The tests were randomized to reduce the unpredictable differences in the observed responses caused by uncontrollable extraneous factors, much like in any statistical design of experiment. Tensile strength, elongation at break, and modulus at 100% are among the responses examined. Equation 2 illustrates how the empirical model to determine the correlation between the variables and each

response Y was developed using a second-degree polynomial equation.

$Y = \beta o + \sum \beta iXi + \sum \beta iiXi^2 + \sum \sum \beta ii\ Xij\ Xij$ (2)

In it, B_o is the intercept coefficient, βi is the linear terms, βii is the squared terms, βij is the interaction terms, and xi and xj are the explicit independent variables. Term Y is the response (yield). The effects of the primary factors and any possible interactions between them on the vulcanization of natural rubber were estimated using analysis of variance (ANOVA).

2.7 Evaluation of the Model and Statistical Analysis

The Design Expert software was used to statistically analyze the experimental design. The statistical significance of the generated model was assessed using multiple linear regression analysis of the experimental data. To examine the significance of the regression coefficient of determination for each effect (linear, quadratic, and interaction) in the model and to evaluate the response model's fit to the data (the lack of fit parameters), analysis of variance (ANOVA) of the model for each response was also carried out. This allowed for the evaluation of the models' significance for additional rationalization. Additionally, modified R^2 and predicted R^2 were used to assess the model's competency.

Table 2: Coded and uncoded levels of independent variables were examined in the CCD.

Coded variable levels	V1(A) Time (min.)	V2 (B) Temperature (°C)	V3 (C) Fiber length (cm)
-1	5.50	145	Short fiber
0	8.50	155	0
+1	11.5	165	Long fiber

V1= Variable 1, V2= VariableV3= Variable 3

Table 3: Experimental Design Matrix

Number of Runs	Type	Time (min)	Temperature(°C)	Fiber length(cm)
1	Factorial	10.00	150	Short
2	Axial	8.50	145	short
3	Center	8.50	155	Long
4	Axial	8.50	145	Long
5	Axial	11.5	155	Long
6	Center	8.50	155	short
7	Factorial	10.00	160	Short
8	Factorial	10.00	160	Long
9	Axial	11.50	155	Short
10	Axial	5.50	155	Long
11	Center	8.50	155	Short
12	Factorial	10.00	150	Long
13	Factorial	7.00	150	Short
14	Axial	5.50	155	Short
15	Center	8.50	155	Long
16	Center	8.50	155	Short
17	Center	8.50	155	Short
18	Center	8.50	155	Long
19	Center	8.50	155	Short
20	Axial	8.50	165	Long
21	Factorial	7.00	150	Long
22	Center	8.50	155	Long
23	Center	8.50	155	Long
24	Factorial	7.00	160	Long
25	Factorial	7.00	160	Short
26	Axial	8.50	165	Short

3. Results and Discussion

3.1 Palmyra Palm Fiber Characterization

The characterization results in Table 3.1 show that the cellulose (%w/w) content of untreated fiber is 58.68±0.66, and for Treated fiber, 61.20±0.211. The moderate Kurkdjian-Hoffman cellulose contents and relatively high lignin contents were indications of high mechanical strength. The cellulose with high lignin content is an indicator of stiffness and low pulp yield. Thus, this fiber would be suitable for composite reinforcement but not for pulp or paper making. This was further confirmed by the cellulose/lignin ratio, which is slightly greater than two (Hansong et al., 2026).

Ash present in lignocelluloses contains silica that has many undesirable effects. Silica blunts cutting machinery, reduces the digestibility of straw, interferes with the pulping process by forming scales on the surface of the reactors, and makes combustion more difficult.

The ash content (%w/w) of the fiber used in this study is 1.67±0.021 for untreated fiber and for treated fiber 1.28±0.87, which were comparable to the best fibers of flax and hemp (1 – 2%) but lower than jute (8%), ramie (5%), and cotton (0%). The reduction in the ash content of the alkali-treated sample may be the result of a reaction between NaOH and any of the inorganic components, for example, silicon to give sodium silicate.

The Hemicellulose content of untreated fiber is 13.94±0.56, and treated fiber is 11.48±2.11. The low hemicellulose content of the plant fiber used in this study implies that its water-absorbing capacity will be low since hemicellulose is the cell wall polymer with the highest water sorption capacity. This is responsible for the high moisture absorption of natural fiber, leading to swelling and the presence of voids, which results in poor mechanical properties and reduces the dimensional stability of the composite (Selvakumar and Omkumar, 2022). This particular property reaffirms the potential of the Palmyra palm fiber used in this study for biocomposite technology.

Since lignin provides fibers with compressive strength, stiffens the fiber, and protects the cellulose and hemicellulose from chemical and physical damage, the biofibres used in this study will be suitable for composite reinforcement because they contain 29.22±0.002 for untreated fiber, while treated fiber is 30.33±0.44. The acid-soluble lignin of the biofibre was comparable to the range obtained for other characterized biofibres. The lignin content of the fibers influences the structure, properties, morphology, flexibility, and rate of hydrolysis. Fibers with higher lignin content appear finer and will be more flexible; thus, they can be used for composite manufacture (Deivayanai et al., 2022).

The moisture content of the untreated fiber is 9.64±0.001, while that of treated fiber is 10.23±0.026. The determination of the moisture content of fibers is very important because fiber dimensions and properties vary with the moisture content (Mohanty *et al.*, 2000). Such properties affected by the moisture content include the degree of crystallinity, crystallite orientation, tensile strength, swelling behavior, and porosity. Also, increased moisture content decreases electrical resistance, and this affects the dimensional stability (Mohanty *et al.*, 2000). The strong hydrophilic nature of plant fibers means that precautions must be taken to improve the water-related dimensional stability of the fibers and to enhance the low compatibility between the fibers and the hydrophobic polymeric matrix (Anteneh et al., 2024).

The high moisture content after the alkalization process is due to the removal of non-cellulose compounds such as waxes; the fibers tend to absorb moisture. This is evident in the study by Nwankwo et al., 2025, where the moisture content for alkali-treated fibers was 5.5% compared to untreated fibers (4.5%).

However, the use of the alkali-treated sample as a composite material decreases its ability to absorb moisture because the fibers get masked with the polyester resin in the laminate with

stronger adhesion, resulting in greater hydrophobicity and less water absorption (C Martínez et al., 2021). It was reported that silane coupling leads to improved properties only in humid environments, due to silane's capacity to reduce fiber moisture absorption.

Table 3.1 Palmyra palm fiber characterization results

S/N	Test	Untreated	Treated
1	Percentage n-hexane/methanol extractives (%w/w)	5.44	N. I.
2	Cellulose (% w/w)	58.68 ±0.66	61.20 ± 0.211
3	Lignin (Klason or acid insoluble) (% w/w)	29.22±0.002	30.33 ± 0.44
4	Hemicellulose (%w/w)	13.94 ± 0.56	11.48 ± 2.11
5	Water content (%)	9.64±0.001	10.23 ± 0.026
6	Ash content (%w/w)	1.67±0.021	1.28 ± 0.87
7	Cellulose/Lignin ratio	>2.0	>2
	ASL- and its derived products (%w/v)		
8i	Ferulic acid (322nm)	0.012	N. I.
8ii	p- coumaric acid (308nm)	0.26 ± 0.05	N. I.
8iii	Vanillin (230nm)	0.0331 ± 0.42	N. I.
8iv	Total Acid Soluble Lignin (ASL %w/v) 205nm	0.321	0.245 ± 0.013

N. I. = Not Identified

3.2 Phytochemical Analysis

The phytochemical analysis of the fiber revealed that alkaline and Silane treatment is necessary due to the presence of these phytochemicals, to remove the lipophilic extractives (gums and waxes) and to remove the polar extractives (proteins, tannins, etc.). Extractives affect the performance of plant fibers in composites.

Table 3.2-Phytochemical analysis results

S/N	Phytochemical	Quantitative
1	Alkaloids	++
2	Flavonoids	-
3	Proteins	-
4	Carbohydrates	++
5	Tannins	+++
6	Oils	-
7	Resins	+

The sign +++ shows relatively high abundance of the compound; ++ shows Moderate presence, and + shows low presence. Palmyra fiber has high abundance of Tannins, moderate Carbohydrates and alkaloids, with low presence of Resins. It has no Flavonoids, proteins, or oils.

3.3 Infrared Position of Various Bonds

Fourier Transform infrared spectrophotometer tells us about the type of functional group present in the sample of fiber chosen for the work and also about the concentration of bands by using values of transmittance.

The results from the FTIR analysis were presented in Table 3.3 (for treated Palmyra palm fiber) and Table 3.4 (for untreated Palmyra palm fiber). The graphs are also presented in Figures 3.1 and 3.2 for untreated and treated fibers, respectively. The FTIR analysis on both samples (treated and untreated Palmyra palm fiber) showed that the fiber contains certain amines, phosphines, alkanes, alkenes, carboxylic acids, ethers, and alcohol compounds (Tables 3.3 and 3.4). The presence of amine and phosphine shows that the fiber is a good one because amine and phosphine are potential antioxidants.

Finally, the most abundant types of bonds on the treated fiber are N-H, P-H, C-H, and C-O. The modes of bonds are stretching and bending.

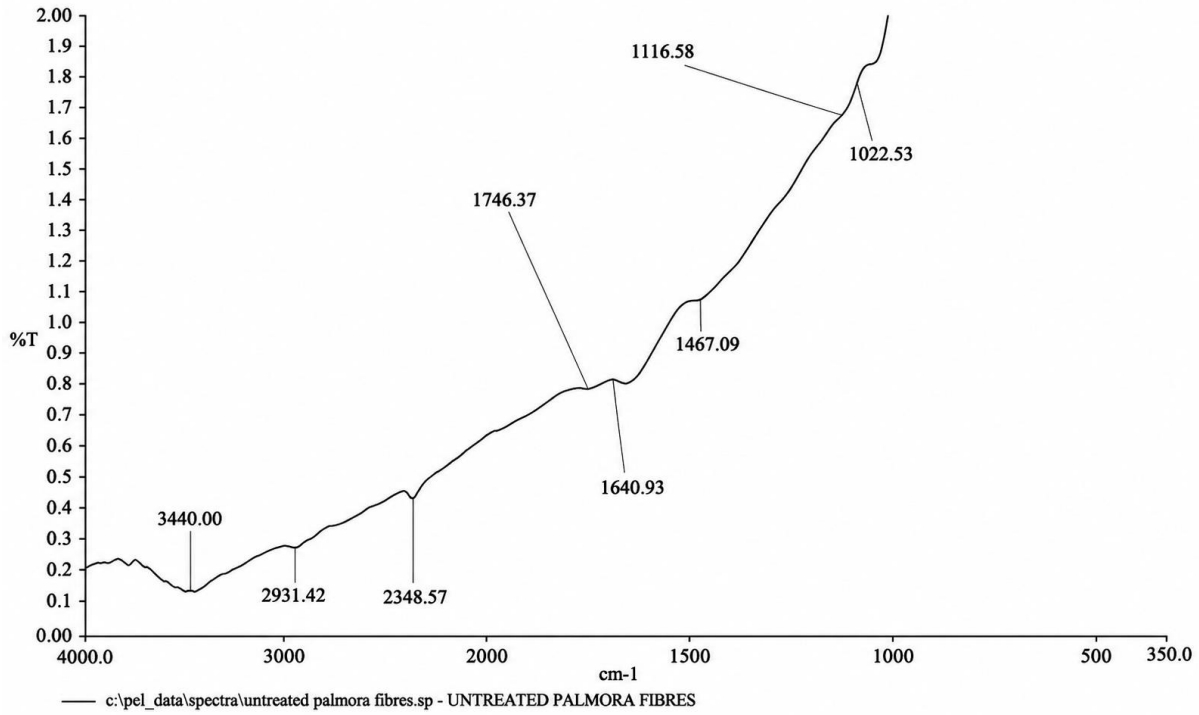

Figure 3.1: Infrared spectra of untreated Palmyra palm fiber

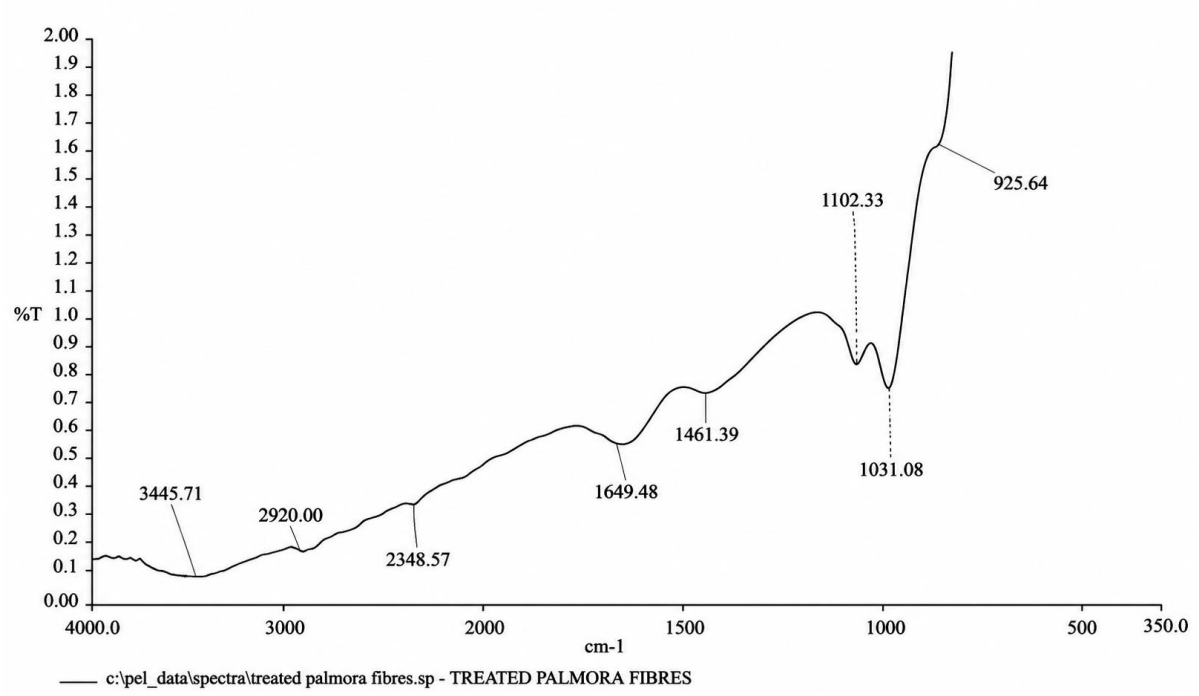

Figure 3.2: Infrared spectra of treated Palmyra palm fiber

Table 3.3 Vibrations of treated Palmyra palm fiber

	Peaks (cm^1)	Bond	Compound type	Mode	Transmittance (%)	Concentration
1.	3445.71	N-H	Amines	stretch	0.01	Medium
2.	2920.00	C-H	Alkanes	Stretch	0.14	Strong
3.	2348.57	P-H	Phosphine	Stretch	0.31	Medium and sharp
4.	1649.48	N-H	Amines	bending	0.52	Broad

5.	1461.39	C-H	Alkanes	Stretch	0.73	Variable
6.	1102.33	C-O	Alcohols,Ethers,carboxylic acids,esters	Stretch	0.76	Strong
7.	1031.08	C-O	Alcohols,Ethers,carboxylic acids,esters	stretch	0.81	Strong
8.	925.64	C-H	C-H	bend	1.71	Strong

Table 3.4 Vibrations of untreated Palmyra palm fiber.

	Peaks (cm^1)	Bond	Compound Type	Mode	Transmittance %	Concentration
1.	3440.00	N-H	Amines	Stretch	0.13	Medium
2.	2931.42	C-H	Alkanes	Stretch	0.24	Strong
3.	2348.57	P-H	Phosphine	Stretch	0.42	Medium and sharp
4.	1746.37	C=O	Aldehydes,Ketones,Carboxylic acids Esters	Stretch	0.74	Strong
5.	1640.93	N-H	Amines	Bend	0.81	Medium
6.	1467.09	C-H	Alkanes	Scissoring and bending	1.12	Variable
7.	1116.58	C-O	Alcohols,Ethers,carboxylic acids,esters	Stretch	1.64	Strong
8.	1022,53	C-O	Alcohols,Ethers,carboxylic acids,esters	Stretch	1.84	Strong

Table 3.5 – 3.9 show the outcomes of the optimization testing of the three factors (vulcanization temperature, duration, and fiber length) on the responses (modulus at 100% elongation, tensile strength, and elongation at break). Table 3.10 displays the surface response quadratic models that were utilized to examine the relationship between the independent factors and the responses. It also included model regression coefficients for evaluating the model's suitability. The model's correlation coefficient values, standard deviation, and acceptable accuracy, a term that quantifies the signal-to-noise ratio were included.

3.4 Impact of vulcanization parameters on the vulcanizate's tensile strength, elongation at break, and modulus.

Using the experimental design, the impact of independent variables (temperature, duration, and fiber length) on the tensile strength was examined, where the findings are presented in Table 4. The vulcanite's tensile strength after a specific amount of time, temperature, and fiber length was reported. The lowest tensile strength reported was for the run N26 (1.5Mpa), whereas the highest tensile strength was for the run N21 (5.8Mpa). The lowest tensile strength was obtained when time was 8.50minutes, temperature 165ºC (highest temperature) and at short length of fiber. On the other hand, the highest tensile strength was obtained at 7 minutes, 150 °C, and long fiber length. The results obtained show that temperature and time of vulcanization have a great effect on the tensile strength of the

vulcanizate. Statistical analyses of the RSM data in Tables 5 – 8 revealed the basis for a quadratic relationship between the response and the vulcanization factors. Table 9 presents the surface response quadratic model that uses CCD to determine the link between the factors and the vulcanizate's tensile strength.

The model's regression coefficients, R^2, adjusted R^2, and forecast R^2 are respectively reported as 0.9122, 0.8708, and 0.7861. The strong R^2 values, which are around unity, show that the proposed model can forecast the vulcanizate's final tensile strength. Additionally, the predictive model's accuracy is confirmed by the tight agreement within these numbers.

Table 3.5: Results of the DOE design matrix

Number of Run	(A) Time (min)	Temperature (°C)	Fiber length (cm)	Tensile strength (Mpa)	Elongation at break (%)	Modulus at 100% (Mpa)
1	10.00	150	Short length	5	727	0.72
2	8.50	145	Short length	5	715	0.75
3	8.50	155	Long length	4.4	712	0.60
4	8.50	145	Long length	5.2	720	0.82
5	11.50	155	Long length	2.8	571	0.53
6	8.50	155	Short length	4.0	695	0.56
7	10.00	160	Short length	2	564	0.48
8	11.50	160	Long length	2.5	579	0.51
9	5.50	155	Short length	2.3	575	0.49
10	8.50	155	Long length	4.4	716	0.65
11	10.00	155	Short length	3.7	635	0.51
12	7.00	150	Long length	5.1	718	0.75
13	5.50	150	Short length	5.5	738	0.76
14	8.50	155	Short length	4.8	718	0.68
15	8.50	155	Long length	4.1	715	0.57
16	8.50	155	Short length	4.6	716	0.60
17	8.50	155	Short length	4.2	705	0.60
18	8.50	155	Long length	3.4	622	0.55
19	8.50	155	Short length	3.8	695	0.52
20	8.50	165	Long length	1.6	525	0.49
21	7.00	150	Long length	5.8	740	0.80
22	8.50	155	Long length	3.8	641	0.56
23	8.50	155	Long length	4	697	0.58
24	7.00	160	Long length	4	689	0.59
25	7.00	160	Short length	3.9	686	0.59
26	8.50	165	Short length	1.5	522	0.5

TABLE 3.6: Tensile Strength (mpa) Analysis of Variance (ANOVA) using the RSM model

Source	Sum of Squares	Degree of Freedom	Mean Squares	F-Value	P-Value
Model	31.36	8	3.92	22.07	<0.0001 (Significant)
A	6.83	1	6.83	38.43	<0.0001
B	22.43	1	22.43	126.26	<0.0001
C	0.025	1	0.025	0.14	0.7143
AB	0.61	1	0.61	3.41	0.0825
AC	0.17	1	0.17	0.94	0.3463
BC	0.000	1	0.000	0.000	1.000
A^2	0.44	1	0.44	2.46	0.1353

B^2	1.18	1	1.18	6.62	0.0915
Residual	3.02	17	0.18	-	-
Lack of fit	1.96	9	0.22	1.63	0.2503 (Not Significant)
Pure error	1.06	8	0.13	-	-
Cor total	34.38	25	-	-	-

Table 3.7: Analysis of Variance (ANOVA) for Elongation at break (%) for RSM Model

Source	**Sum of Squares**	**Degree of Freedom**	**Mean Squares**	**F-Value**	**P-Value**
Model	1.046E+005	8	13069.91	15.26	<0.0001 (Significant)
A	29470.04	1	29470.04	34.41	<0.0001
B	58115.04	1	58115.04	67.86	<0.0001
C	81.38	1	81.38	0.095	0.7616
AB	4950.12	1	4960.12	0.78	0.0279
AC	0.37	1	0.37	4.379E-004	0.9835
BC	18.37	1	18.37	0.021	0.8853
A^2	3873.72	1	3873.72	4.52	0.0484
B^2	10754.29	1	10754.29	12.56	0.0025
Residual	14559.31	17	856.43	-	-
Lack of fit	3197.31	9	355.26	0.25	0.9730 (Not Significant)
Pure error	11362.00	8	1420.25	-	-
Cor total	1.191E+005	25	-	-	-

Table 3.8: Modulus at 100% elongation (Mpa) Analysis of Variance (ANOVA) for RSM Model

Source	**Sum of Squares**	**Degree of Freedom**	**Mean Squares**	**F-Value**	**P-Value**
Model	0.23	8	0.028	13.22	<0.0001(Significant)
A	0.034	1	0.034	15.66	<0.0001
B	0.17	1	0.17	78.89	<0.0001
C	2.215E-003	1	2.215E-003	1.03	0.3249
AB	1.250E-003	1	1.250E-003	0.58	0.4567
AC	1.067E-003	1	1.067E-003	0.49	0.4913
BC	1.667E-003	1	1.667E-003	0.77	0.3914
A^2	2.039E-003	1	2.039E-003	0.95	0.3444
B^2	0.018	1	0.018	8.33	0.0102
Residual	0.037	17	2.155E-003	-	-
Lack of fit	0.028	9	3.098E-003	2.83	0.0790 (Not Significant)
Pure error	8.760E-003	8	1.095E-003	-	-
Cor total	0.26	25	-	-	-

Table 3.9: DOE design matrix, actual and predicted values for the responses

Standard Order	Time (min)	Temp. (°C)	Fiber Length (cm)	Actual values for tensile strength (Mpa)	Predicted values for tensile strength (Mpa)	Actual values for elongation at break (%)	Predicted values for elongation at break (%)	Actual values for M100 (Mpa)	Predicted values for M100 (Mpa)
1	7.00	150	Short	5.50	5.16	738.00	726.78	0.76	0.71
2	10.00	150	Short	5.00	4.47	727.00	706.69	0.72	0.64
3	7.00	160	Short	3.90	3.77	686.00	676.36	0.59	0.58
4	10.00	160	Short	2.00	1.99	564.00	556.78	0.48	0.47

5	5.50	155	Short	4.80	4.95	718.00	724.22	0.68	0.69
6	11.50	155	Short	2.30	2.48	575.00	584.56	0.49	0.51
7	8.50	145	Short	5.00	5.40	715.00	730.06	0.75	0.80
8	8.50	165	Short	1.50	1.53	522.00	529.72	0.50	0.50
9	8.50	155	Short	4.20	4.11	705.00	691.17	0.60	0.57
10	8.50	155	Short	4.00	4.11	695.00	691.17	0.56	0.57
11	8.50	155	Short	3.70	4.11	635.00	691.17	0.51	0.57
12	8.50	155	Short	3.80	4.11	695.00	691.17	0.52	0.57
13	8.50	155	Short	4.60	4.11	716.00	691.17	0.60	0.57
14	7.00	150	Long	5.80	5.05	740.00	721.74	0.80	0.73
15	10.00	150	Long	5.10	4.70	718.00	701.16	0.75	0.69
16	7.00	160	Long	4.00	3.67	689.00	674.82	0.59	0.57
17	10.00	160	Long	2.50	2.22	579.00	554.74	0.51	0.48
18	8.50	155	Long	4.40	4.68	716.00	721.18	0.65	0.68
19	11.50	155	Long	2.80	2.88	571.00	580.52	0.53	0.56
20	8.50	145	Long	5.20	5.46	720.00	723.02	0.82	0.86
21	8.50	165	Long	1.60	1.59	525.00	529.63	0.49	0.49
22	8.50	155	Long	4.40	4.17	712.00	687.63	0.60	0.59
23	8.50	155	Long	4.00	4.17	697.00	687.63	0.58	0.59
24	8.50	155	Long	3.40	4.17	622.00	687.63	0.55	0.59
25	8.50	155	Long	4.10	4.17	715.00	687.63	0.57	0.59
26	8.50	155	Long	3.80	4.17	641.00	687.63	0.56	0.59

Table 3.10: Adequacy of the model

Quadratic equations (A = Time, B= Temperature, C = Fiber length)	R^2	Adjusted R^2	Predicted R^2	Standard deviation	Adequate Precision
Tensile Strength (Mpa) = 4.14-0.53A-0.97B	0.9122	0.8708	0.7861	0.42	15.842
Elongation at Break (%) = 689.40-35.04A-49.21B-24.87AB-9.19A^2-15.32B^2	0.8778	0.8203	0.7958	29.26	11.637
Modulus at 100% elongation (Mpa) = 0.58-0.038A-0.084B+0.02B^2	0.8615	0.7964	0.6185	0.046	14.230

The model's importance within the experimental window is indicated by the remarkable connection between the anticipated and actual tensile strengths, as shown in Figure 3.3. The RSM contour is displayed in Figure 3.4. As revealed, the model's repeatability was 0.42, and a minimal standard deviation suggests that it is repeatable. Additionally, the reported model's appropriate precision was quite high (15.842); a better model will have a value greater than 4, indicating the model's suitability for navigating the design space once more.

Significant effects are defined as coefficients with P-values less than 0.05. The quadratic model's high Fischer variance value (F-value) (22.07) and P value (<0.0001) suggested that this model is important. The contour plot and the 3D surface graphs show that the tensile strength increases as the time decreases from 10 minute to 7 minutes and temperature decreases from 160°C to 150°C (Figure 3).

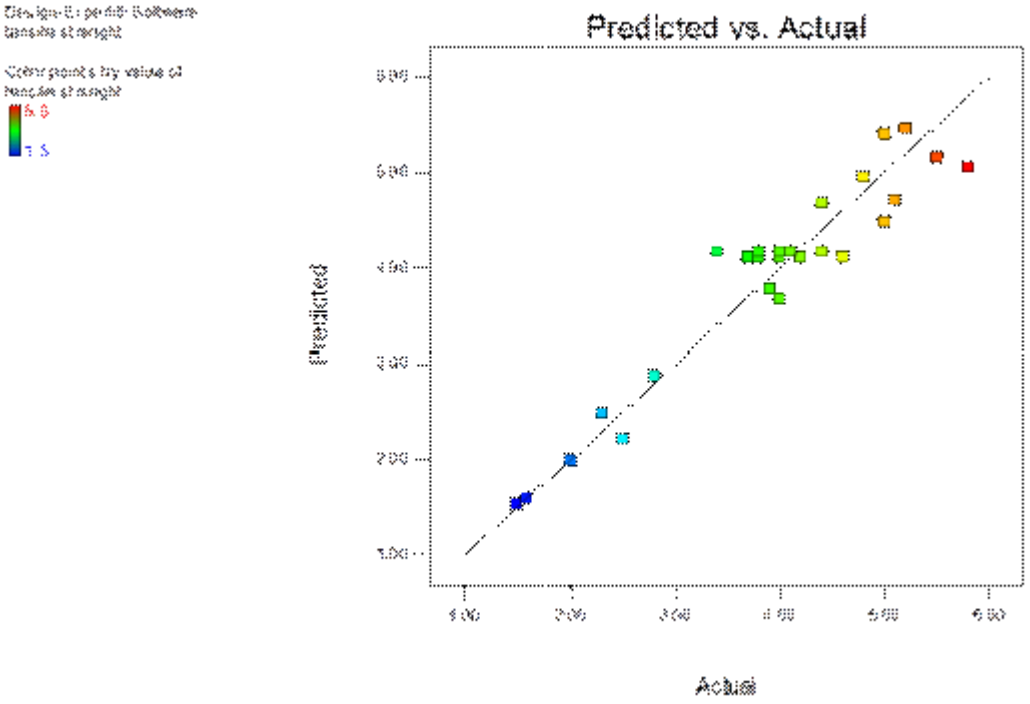

Fig. 3.3 predicted versus actual for tensile strength

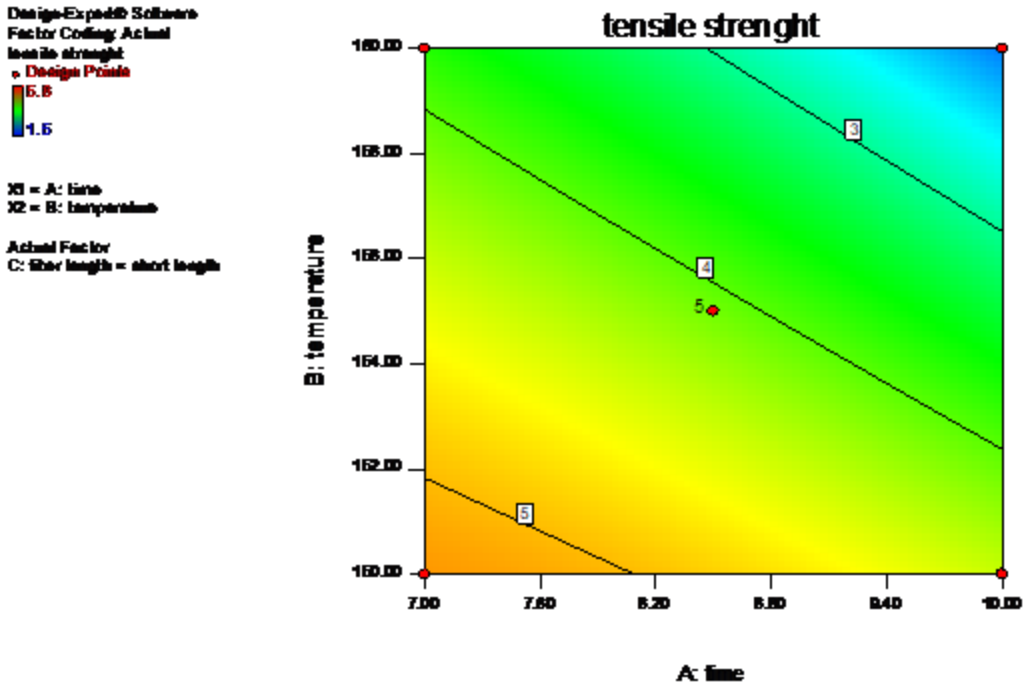

Fig. 3.4 Response surface contour for temperature and time interaction effects on the tensile strength.

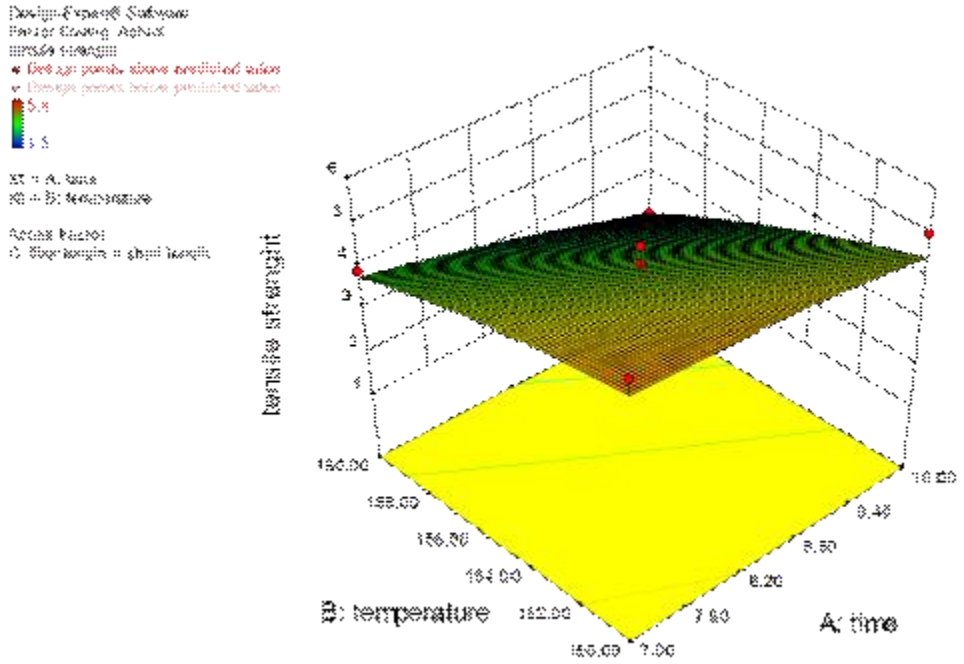

Fig 3.5 Three-dimensional response surface plots showing how temperature and time affect tensile strength.

For the second response (elongation at break), RSM graphs are presented in Figures 3.6 – 3.8. Figures 3.6 and 3.7 show the model graphs of the design. The contour plot and the 3D surface graphs show that the elongation at break increases as time and temperature reduce. Table 3.10 displays the regression coefficients R^2, adjusted R^2, and forecast R^2 for the model, which are 0.8778, 0.8203, and 0.7958, respectively. The model can predict the eventual elongation upon vulcanizate break, as indicated by the high R^2 values near unity. The model appears to be significant based on its F-value of 15.26.A "Model F-Value" this large has a 0.01% probability of being caused by noise. Model terms are considered significant when "Prob > F" values are less than 0.0500. A, B, AB, A^2, and B^2 are important model terms in this instance. The model terms are not significant if the value is more than 0.1000. Model reduction may help the model if there are a lot of unimportant model terms. The "Lack of Fit F-value" of 0.25 indicates that, in comparison to the pure error, the Lack of Fit is not significant. A "Lack of Fit F-value" this high has a 97.30% probability of being caused by noise. Since adequate model fitting is desirable, a non-significant loss of fit is beneficial.

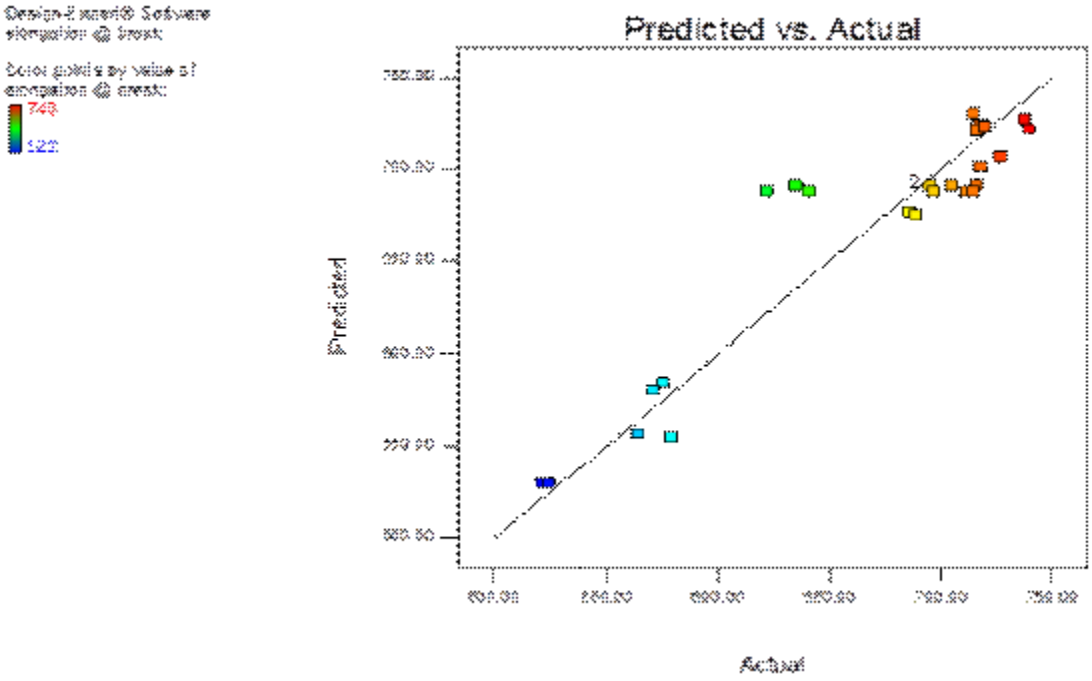

Fig. 3.6. Predicted versus actual for elongation at break

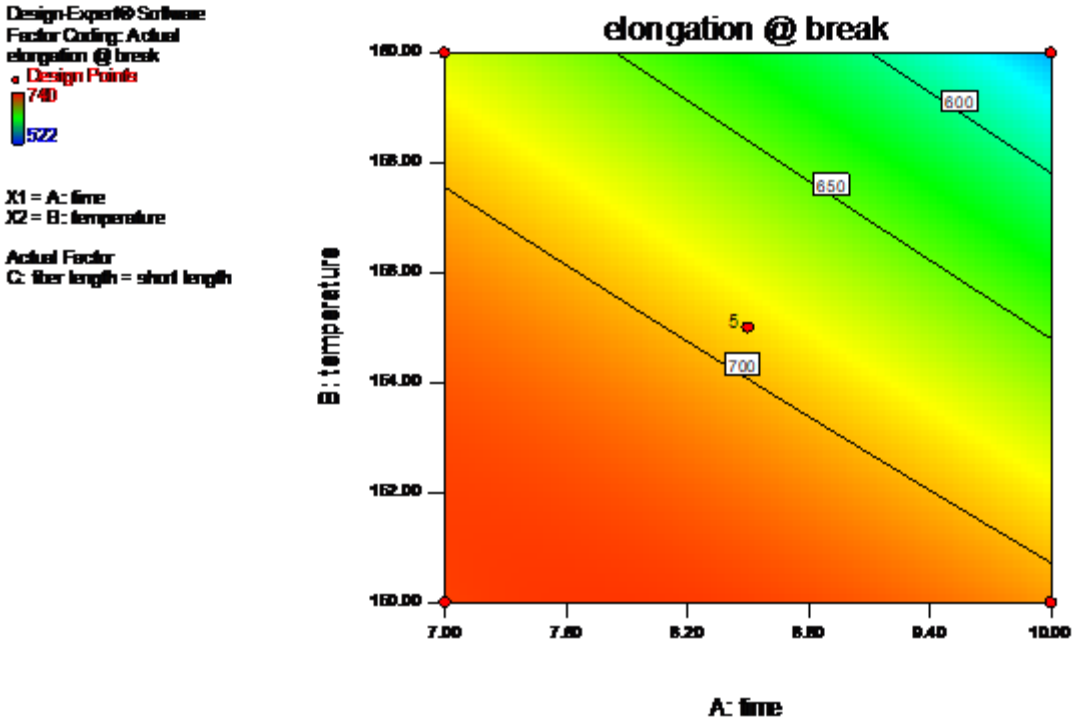

Fig 3.7. Response surface contour for the temperature versus time interaction effect on elongation at break

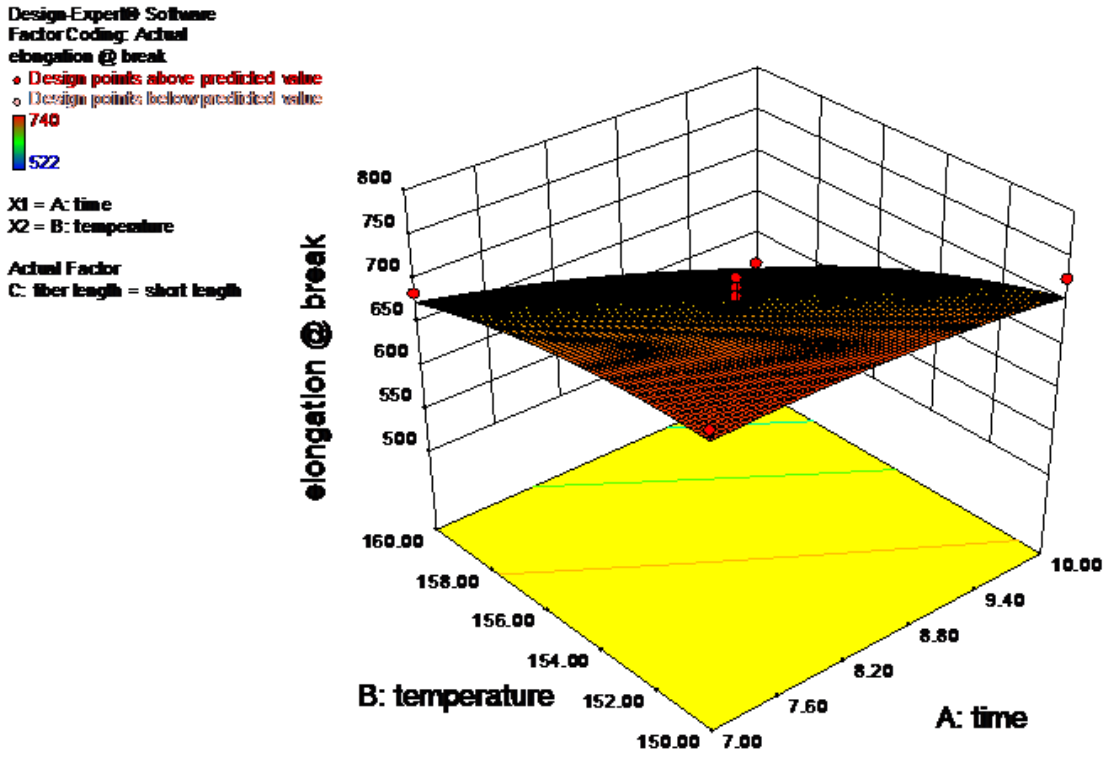

Fig 3.8. Three-dimensional response surface plots showing how temperature and time affect tensile strength.

Table 3.10 displays the statistical analysis derived from the analysis of variance (ANOVA) for the response reduced quadratic model for the third response modulus at 100% elongation. A very high significance for the regression model is demonstrated by the Fischer F-test (F model = 13.22) with a very low probability value (Prob > F) = 0.0500. This is good because it shows that the model's terms have a big impact on the answer. A "Model F-Value" this large has a 0.01% chance of occurring owing to noise, according to the value of $P < 0.0001$.A, B, and B^2 are important model terms in this instance.

The model terms are not significant if the value is greater than 0.1000. Model reduction could make the model better if there are a lot of unnecessary model terms. The "Lack of Fit F-value" of 2.83 indicates that noise has a 7.90% probability of causing a "Lack of Fit F-value" this high. The "Adj R-Squared" of 0.7964 and the "Pred R-Squared" of 0.6185 agree fairly well. Fig. 3.9 illustrates the link between the response's actual and expected values. It is evident that the projected and actual values align reasonably well.

"Adeq Precision" is a signal-to-noise ratio measurement. The ideal ratio is more than 4. This model ratio of 14.230 shows that the signal is sufficient. Navigating the design space is possible using this paradigm. Figures 3.10 and 3.11 show the model graphs of the design. The contour plot and the 3D surface graphs show that the M100 increases as time and temperature decrease. The residual's normal probability curve, displayed in Fig. 3.10, was used to further analyze the modulus at 100%. The errors are negligible and distributed normally in a straight line, according to the residual's normal probability plot.

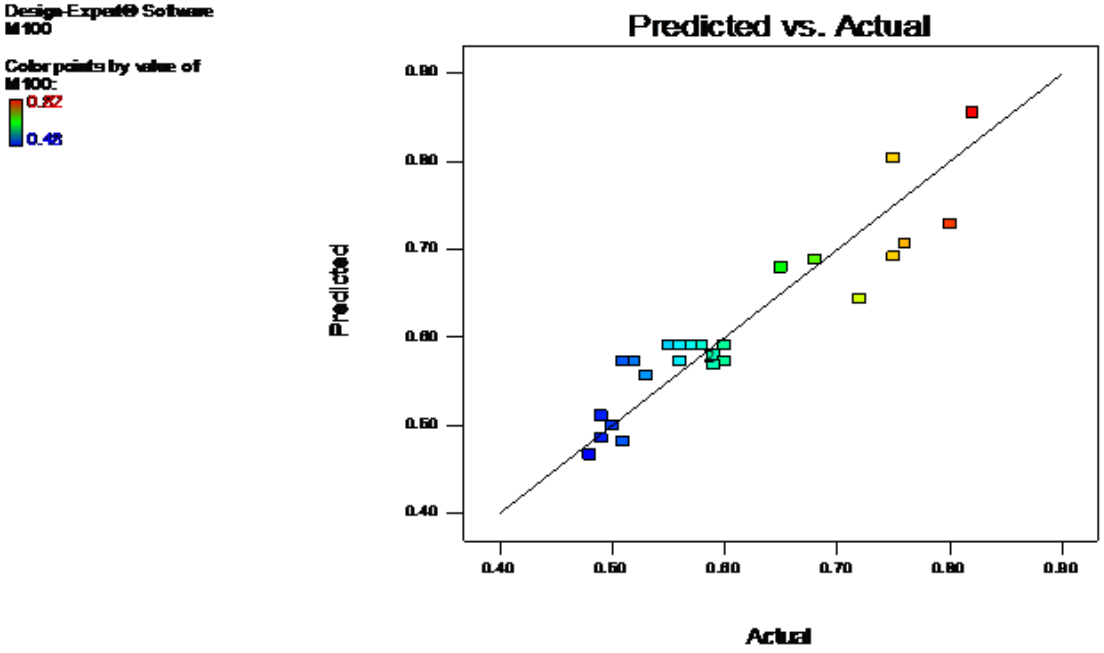

Fig. 3.9: Predicted versus actual Modulus at 100% elongation

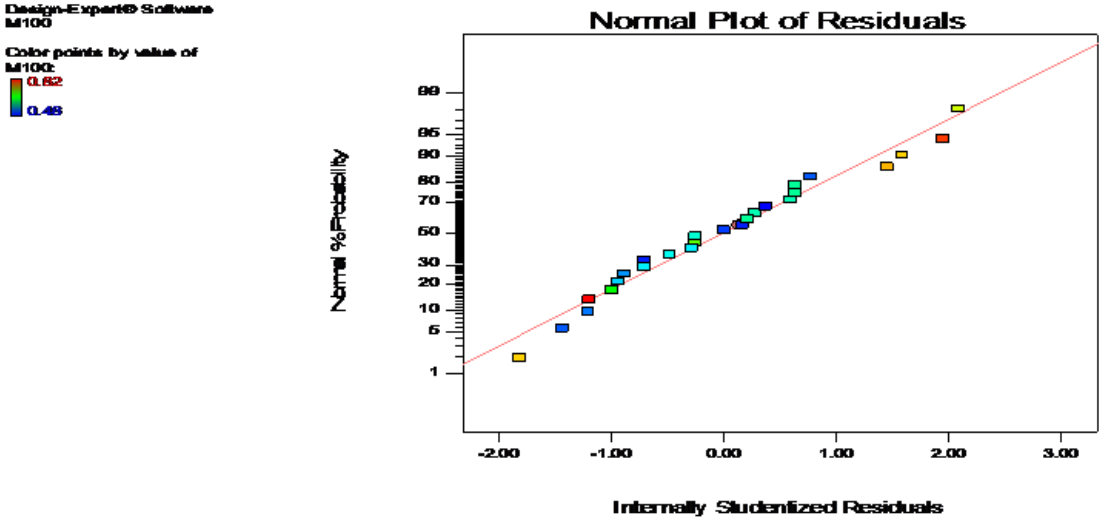

Fig 3.10. Normal probability curve of residual [Modulus at 100% elongation]

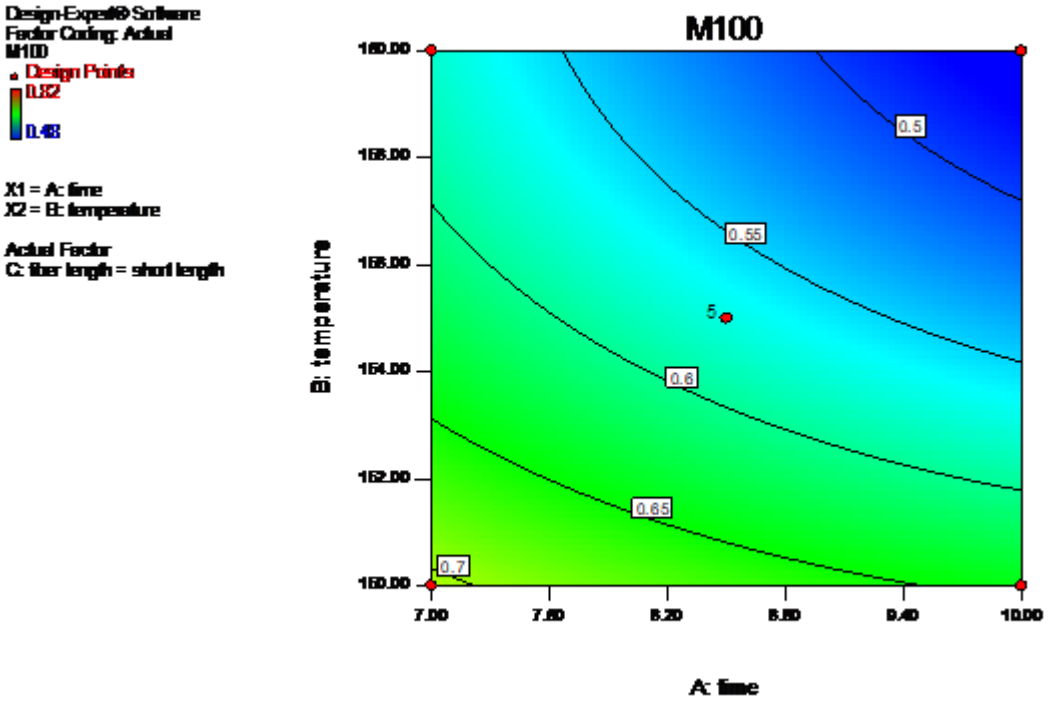

Fig 3.11. Response surface contour of the interactive effect of time and temperature on the modulus at 100% elongation.

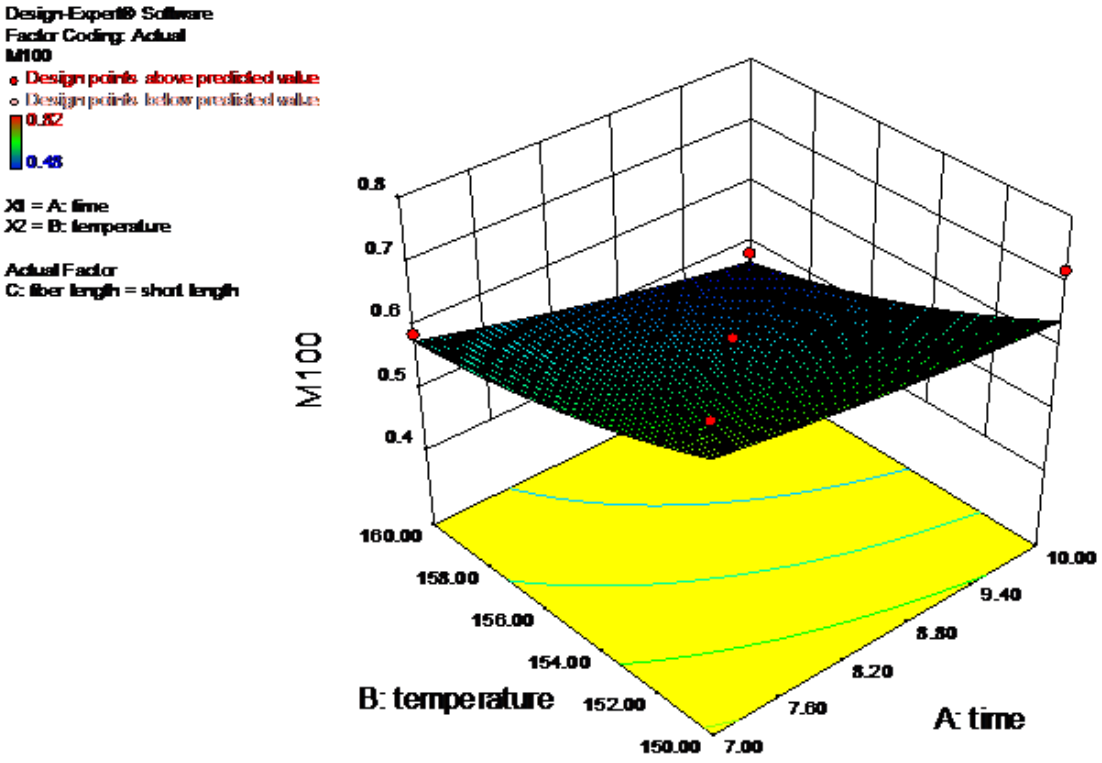

Fig 10. Three-dimensional response surface plots of the interaction of time and temperature for modulus at 100% elongation.

3.5. Optimization of vulcanization process using Palmyra palm fiber and validation of the model

Optimization of the process was performed

using Design-Expert 8.0.7.1 trial version to maximize the vulcanization process parameters. The optimal vulcanization conditions for obtaining a high-quality product were extracted by the Design-Expert software. The optimal values selected by the model are; tensile strength, 5.05Mpa, elongation @ break, 721.74% and M100, 0.73 MPa, at the following process parameters, time, 7.00, minutes, temperature, 150 °C, and long fiber length.

To validate the model, confirmatory experiments were conducted using combinations of independent variables that were within the experimental region but were not included in the original experimental design. The results obtained were as follows; tensile strength, 5.4Mpa, elongation at break, 739% and M100, 0.7. The predicted and experimental values were in good agreement. These validations confirmed the suitability of the design chosen, method of sample preparation, and property evaluation.

4. Conclusion

Palmyra palm fiber was used as a filler to optimize the vulcanization process of natural rubber using a central composite design of surface response method. Three vulcanization parameters (temperature, duration, and fiber length) were examined in relation to tensile strength, elongation at break, and modulus at 100%. The vulcanization variables were correlated with the three responses using two quadratic models and one linear model. The models' statistical significance for predicting each response under study was revealed by the models' analysis of variance (ANOVA). In order to maximize the vulcanization process, process optimization was carried out. It was discovered that the experimental results for the corresponding tensile strength, elongation at break, and modulus at 100% agreed adequately with the linear and quadratic vulcanization models. Optimum conditions used for vulcanization were: tensile strength, 5.05Mpa, elongation at break, 721.74%, and M100, 0.73Mpa at the following process parameters: time, 7.00 minutes, temperature, 150°C, and long fiber length.

REFRENCES

Alshabatata, N., & Abouel-Kasem, A. (2021). The effects of sulfur content on the mechanical properties of nitrile butadiene rubber with different aging conditions. *Jordan Journal of Mechanical and Industrial Engineering, 15*(4), 387–393.

Anteneh, G., Pieter, D. W., & Tamene, A. D. (2024). Surface modification of bamboo fibers through alkaline treatment: Morphological and physical characterization for composite reinforcement. *Journal of Engineered Fibers and Fabrics, 19*(5), 1–13.

Bhunia, A. K., Mondal, D., Mondal Parui, S., & Mondal, A. K. (2023). Characterization of a new natural novel lignocellulose fiber resource from the stem of Cyperus platystylis R.Br. *Scientific Reports, 13*, Article 9699.

Chai, A. B., Kamaruddin, S., Yeow, T. K., Ing, K., Tay, B. J. H., & Ying, C. S. (2016). The effect of oil palm fiber/eggshell powder loading on the mechanical properties of natural rubber composites. *ARPN Journal of Engineering and Applied Sciences, 11*(1), 128–134.

Chimekwene, C. P., Fagbemi, E. A., & Ayeke, P. O. (2012). Mechanical properties of plantain empty fruit bunch fiber reinforced epoxy composite. *International Journal of Research in Engineering, IT and Social Sciences, 2*(6), 86–94.

Deivayanai, V. C., Yaashikaa, P. R., Senthil Kumar, P., & Rangasamy, G. (2022). A comprehensive review on the biological conversion of lignocellulosic biomass into hydrogen: Pretreatment strategy, technology advances and perspectives. *Bioresource Technology, 365*, Article 128166.

Elhousari, A. M., Rashad, M., Elsheikh, A. H., & Dewidar, M. (2021). The effect of rubber powder additives on mechanical properties of polypropylene glass-fiber-reinforced composite. *Mechanical Sciences, 12*, 461–469.

Ghani, H., Abd Karim, S. F., Ramli, R., Musa, M., & Jaapar, J. (2018). Effect of bio fillers

on mechanical properties of natural rubber latex films. *Key Engineering Materials, 797*, 249–254.

Hema Aditya, P., Siva Kishore, K., & Krishna Prasad, D. V. V. (2017). Characterization of natural fiber reinforced composites. *International Journal of Engineering and Applied Sciences, 4*(6).

Kazemi, H., Mighri, F., & Rodrigue, D. (2022). A review of rubber biocomposites reinforced with lignocellulosic fillers. *Journal of Composites Science, 6*(7), Article 183.

Kathiresan, S., & Meenakshisundaram, O. (2022). Effect of alkali treated cellulose fibers and human hair on FTIR and tensile properties for composite material application. *SN Applied Sciences, 4*, Article 74. https://doi.org/10.1007/s42452-022-04946-9

Mohanty, A. K., Khan, M. A., & Hinrichsen, G. (2000). Influence of chemical surface modification on the properties of biodegradable jute fabrics polyester amide composites. *Composites Part A: Applied Science and Manufacturing, 31*(2), 143–150.

Nwabanne, J., Igbokwe, P., & Ezeonyebuchi, E. (2015). Effect of palmyra palm fiber filler on properties of natural rubber vulcanizate. *World Journal of Engineering, 11*(6), 565–574.

Nwankwo, C., Mahachi, J., Olukanni, D., & Musonda, I. (2025). Alkali treatment of flax fibres: Effects on tensile strength, thermal performance, and moisture absorption. *Composite Interfaces, 32*(9), 1329–1346. https://doi.org/10.1080/09276440.2025.2467700

Ondrušová, D., Božeková, S., Buňová, L., Pajtášová, M., Labaj, I., Dubec, A., & Vršková, J. (2018). Modification of alternative additives and their effect on the rubber properties. *MATEC Web of Conferences, 157*, Article 07007.

Roy, K., Debnath, S. C., Tzounis, L., Pongwisuthiruchte, A., & Potiyaraj, P. (2020). Effect of various surface treatments on the performance of jute fibers filled natural rubber (NR) composites. *Polymers, 12*(2), Article 369.

Seisa, K., Chinnasamy, V., & Ude, A. U. (2022). Surface treatments of natural fibres in fibre reinforced composites: A review. *Fibres & Textiles in Eastern Europe, 151*(2), 82–89.

Suárez, C. M., Montejo, P. R., & Junco, O. G. (2021). Effects of alkaline treatments on natural fibers. *Journal of Physics: Conference Series, 2046*, Article 012056.

Wang, Q., Zhang, Y., Liang, W., Wang, J., & Chen, Y. (2020). Effect of silane treatment on mechanical properties and thermal behavior of bamboo fibers reinforced polypropylene composites. Journal of Engineered Fibers and Fabrics, 15, 1–10.

Wu, H., Zhang, J., Song, Y., Jia, D., Sun, G., & Wang, C. (2026). Effect of alkali treatment and silane functionalization on cellulose fibers: Experimental investigation, mechanism and molecular dynamics simulation. *Applied Surface Science, 716*, Article 164716.